Archives of Materials Science and Engineering

Volume 65
Issue 2
February 2014
Pages 77-86

International Scientific Journal
published monthly by the
World Academy of Materials
and Manufacturing Engineering

Computer-assisted analysis of changes in the microstructure of P92 steel after exposure at elevated temperature

A. Zieliński [a,*], J. Dobrzański [a], G. Golański [b], M. Sroka [c]

[a] Institute for Ferrous Metallurgy, ul. K. Miarki 12, 44-100 Gliwice, Poland
[b] Institute of Materials Engineering, Czestochowa University of Technology, ul. Armii Krajowej 19, 42-200 Częstochowa, Poland
[c] Division of Materials Processing Technology, Management and Computer Techniques in Materials Science, Institute of Engineering Materials and Biomaterials, Silesian University of Technology, ul. Konarskiego 18a, 44-100 Gliwice, Poland
* Corresponding e-mail address: azielinski@imz.pl

Received 23.11.2013; published in revised form 01.02.2014

ABSTRACT

Purpose: The purpose of the work was to analyse the components of X10CrWMoVNb9-2 (P92) steel in initial state and after long-term annealing for up to 100,000 h at 600 and 650°C.

Design/methodology/approach: The material for investigation was X10CrWMoVNb9-2 (P92) steel in the form of a Ø160x40mm tube. The images of microstructure were recorded using the scanning electron microscopy. The quantitative analysis of precipitates was carried out using the image analysis system NIKON EPIPHOT200 & LUCIA G v.5.03.

Findings: The investigations of microstructure and the quantitative analysis of precipitates in the tested steel in initial state and after long-term annealing allowed the impact of temperature and time on stability of the microstructure of the tested steel to be evaluated.

Practical implications: The presented method can be used for evaluation and qualification of structural changes in power station boiler components operating under creep conditions.

Originality/value: The presented results of changes in the structure and in the precipitation processes are applied to evaluation of the condition of the elements in further industrial service.

Keywords: Microstructure; Long-term annealing; Hardness; X10CrWMoVNb9-2 (P92) steel

Reference to this paper should be given in the following way:

A. Zieliński, J. Dobrzański, G. Golański, M. Sroka, Computer-assisted analysis of changes in the microstructure of P92 steel after exposure at elevated temperature, Archives of Materials Science and Engineering 65/2 (2014) 77-86.

METHODOLOGY OF RESEARCH, ANALYSIS AND MODELLING

1. Introduction

The construction and operation of boilers with supercritical parameters has resulted in commencement of extensive research on steels for critical components of boilers, carried out jointly by boiler manufacturers and research bodies. In particular, it concerns critical components working under supercritical temperature and stress conditions. The effect of this research is numerous studies concerning functional properties of new-generation steels used under creep conditions [1-12]. The designers expect reliable steel products with guaranteed functional properties that would allow using them for boiler components to be operated under creep conditions for min. 200 thousand hours. In turn, the diagnostics and periodical inspections of these materials during the operation and tools made of them require knowledge of changes in functional properties with time of their service [13-16]. Therefore, conducting a set of investigations to allow building steel characteristics based on investigations of mechanical properties and microstructure is so important [17-28].

The X10CrWMoVNb9-2 (P92) steel was developed by modification of chemical composition of steels containing approx. 9%Cr, which have been used in the power industry so far. This steel is characterised by high mechanical properties; among other things, its creep strength is higher by approx. 20-25% than that of the steels used so far.

Long-term impact of elevated temperature during the operation of pressure equipment and systems brings about changes in the microstructure of the material resulting in reduction of mechanical properties. These changes determine the life time of components, which are now designed for 200,000 hours of operation. However, it does not mean that failure-free operation is ensured for such a long time. Therefore, the diagnostic works and inspections, and possible repairs are carried out during the boiler's lifetime to ensure safe and failure-free operation of power units.

In cooperation with other research centres (Silesian University of Technology, Czestochowa University of Technology, AGH University of Science and Technology in Krakow) as well as the boiler factories Rafako S.A. and SEFKAO S.A. – the leading manufacturers of boilers, the Institute for Ferrous Metallurgy performs the works on the advance and verification testing of new-generation steels for the power industry [2,9,10,17,24,31,32].

This study presents the results of investigations on the components of P92 steel microstructure that affect its stability. These investigations included the analysis of the microstructure and quantitative analysis of precipitates. Steel in initial state and after long-term exposure at elevated temperature was subject to investigation.

The developed P92 steel characteristics with regard to the above-mentioned investigations are used in the assessment of changes in functional properties of the material of elements working under creep conditions.

2. Research methodology, material for investigation

The material for investigation was X10CrWMoVNb9-2 (P92) steel in as-received (initial) state and after long-term exposure at elevated temperature. Long-term term annealing was carried out at 600 and 650°C for up to 100,000 hours.

The microstructure investigations were carried out with Inspect F scanning electron microscope (SEM) on conventionally prepared metallographic microsections etched with ferric chloride.

The quantitative analysis of precipitates was carried out using the image analysis system NIKON EPIPHOT200 & LUCIA G v.5.03. The scale marker as shown in the photos was used for calibration of the image analysis system. Calibration coefficient: 1 pixel= 0.040 μm. A measuring frame of 1020 x 940 pixels was applied on every analysed photo.

Material condition was evaluated based on the diagram of changes in microstructure after long-term service at elevated temperature [30].

The chemical composition of the tested steel is summarised in Table 1.

Table 1.
Material for investigation – chemical composition of P92 steel with reference to the requirements [29]

Steel grade	Element contents, wt%												
	-	C	Mn	Si	P	S	Cr	Mo	V	W	Nb	B	N
P92	Tested material	0.10	0.45	0.17	0.01	0.01	9.26	0.47	0.20	1.95	0.059	0.009	0.04
	according to [29]	0.07-0.13	0.30-0.60	max 0.50	max 0.02	max 0.01	8.5-9.5	0.30-0.60	0.15-0.25	1.5-2.0	0.04-0.09	max 0.006	0.03-0.07

3. Research results and discussion

3.1. Microstructure of P92 steel

In its initial state, the P92 steel is characterised by the microstructure with predominating tempered lath martensite and numerous precipitates.

In the microstructure of the tested steel, there was lath martensite substructure with elongated sub-grains and high density of dislocation as well as polygonised substructure of ferrite grains.

The tempered martensite microstructure with numerous precipitates is typical of this group of steels [9]. The examples of microstructures of the tested steel in initial state are shown in Figures 1 and 2.

Fig. 1. Microstructure of P92 steel in initial state observed using TEM

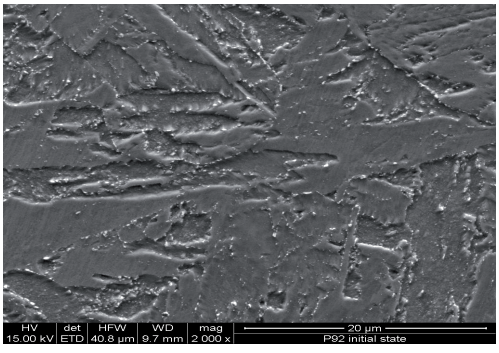

Fig. 2. Microstructure of P92 steel in initial state observed using SEM

The identification of precipitates revealed the existence of the following types of precipitates in the tested steel in initial state: MX and $M_{23}C_6$. The MX – VN and NbX precipitates were observed mainly inside grains – at the dislocations and subgrain boundaries, while $M_{23}C_6$ carbides were revealed at the former austenite grain boundaries and at the martensite lath boundaries [5].

The literature data [3, 5] also indicate that there may be complex precipitates in the tested steel, referred to as the "V-wings". These precipitates consist of a spherical NbX precipitate and VX lamellar precipitates that nucleate on them. However, precipitates of this type were not observed in the tested steel.

The microscopic observations revealed no essential changes in the microstructure of the tested steel after annealing at 600 and 650°C for up to 1000 h (Figs. 3a,b).

a)

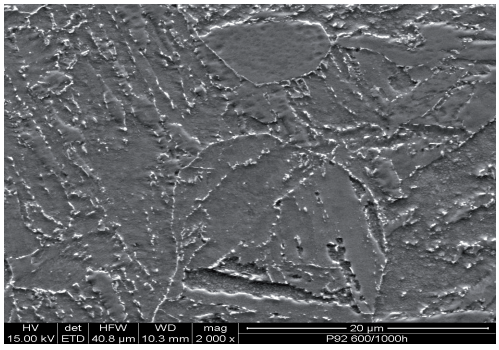

b)

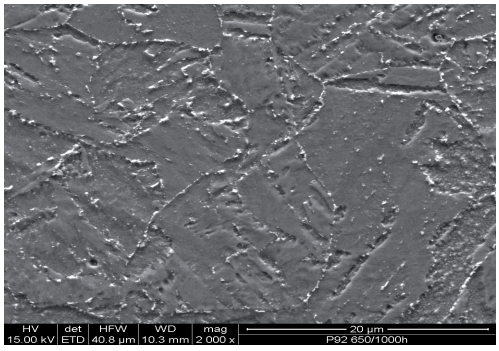

Fig. 3. Microstructure of P92 steel after annealing for 1,000 h at: a) 600°C; b) 650°C, SEM

The visible changes in the microstructure, as compared to the initial state, can be observed on samples annealed for 10,000 hours. The characteristic microstructure images after annealing at 600 and 650°C for 10,000, 30,000, 70,000 and 100,000 h are shown in Figures 4-7.

a)

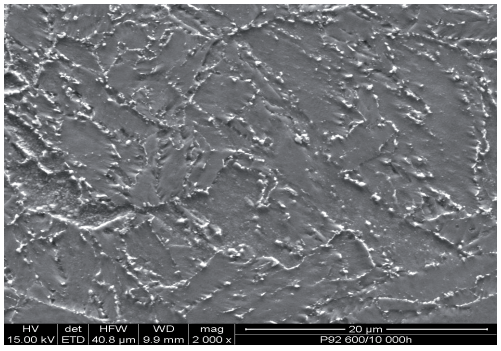

b)

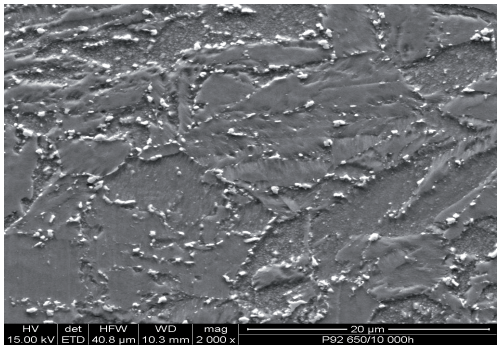

Fig. 4. Microstructure of P92 steel after annealing for 10,000 h at: a) 600°C; b) 650°C, SEM

The increase in the size of precipitates was found after this time of annealing. As it should have been expected, their size was bigger after long-term annealing at 650ºC. In the microstructure of P92 steel after 10,000 h annealing, the effects of further progressing processes related to martensite tempering – softening of matrix can be observed. The result of these processes is bigger and more densely arranged $M_{23}C_6$ carbide precipitates at the former austenite grain boundaries and on martensite laths. In addition to $M_{23}C_6$ carbides at the grain boundaries, the Laves phase precipitates is observed too [5,9]. The annealing at 650°C contributes to local decay of the lath structure of tempered martensite.

The annealing for up to 30,000 h resulted in local decay of the lath structure of tempered martensite areas at test temperature of 600°C (Fig. 5a). The annealing at 650°C resulted in further progressing decay of the lath structure of tempered martensite microstructure (Fig. 5b). This microstructure was characterised by still preserved martensitic microstructure with numerous different size precipitates at the former austenite grain and martensite lath boundaries.

a)

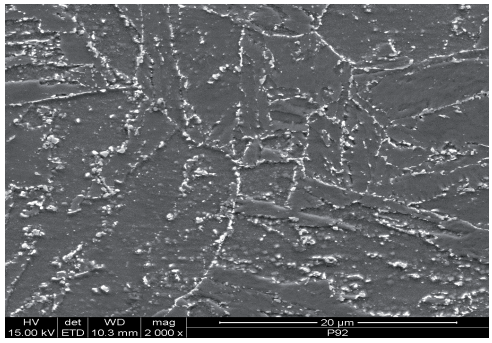

b)

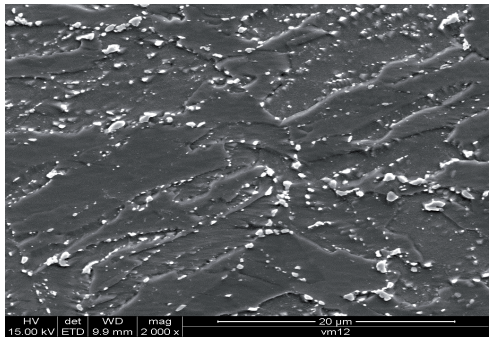

Fig. 5. Microstructure of P92 steel after annealing for 30,000 h at: a) 600°C; b) 650°C, SEM

a)

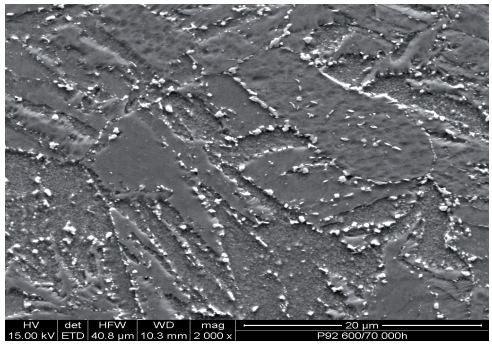

b)

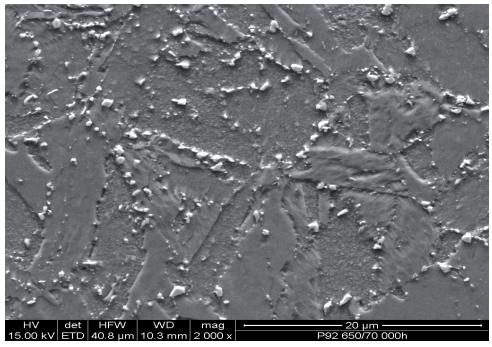

Fig. 6. Microstructure of P92 steel after annealing for 70,000 h at: a) 600°C; b) 650°C, SEM

As compared to the microstructure observed for the same duration of annealing and temperature of 600°C (Fig. 5a), the difference in the size of existing precipitates is noticeable (Fig. 5b). In both the analysed microstructures, areas were observed where the amount of precipitates at the grain boundaries was so high that they formed the so-called continuous network of precipitates.

The extension of the duration of annealing at 600°C up to 70,000 h revealed the increase in the size of precipitates (Fig. 6a), while the image of the microstructure of the tested steel annealed at test temperature of 650°C for 70,000 h shows, in addition to the coagulation of precipitates, further decay of the martensite lath structure (Fig. 6b). This microstructure is characterised by partially degraded areas of martensite with precipitations of large carbides at the former austenite grain boundaries, martensite laths and inside grains.

a)

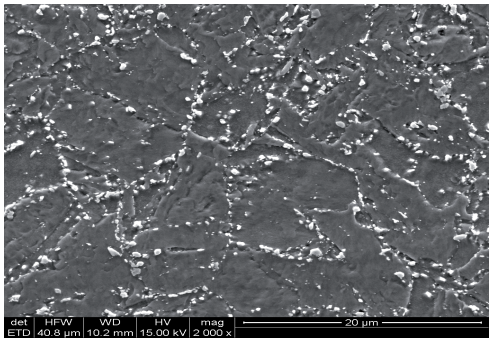

b)

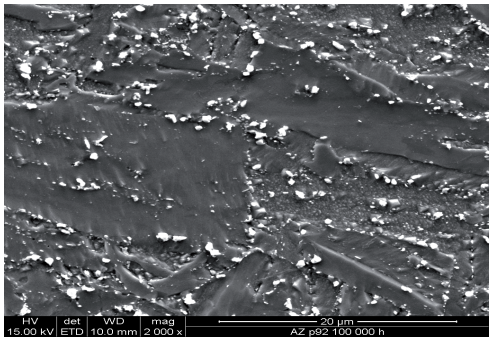

Fig. 7. Microstructure of P92 steel after annealing for 100,000 h at: a) 600°C; b) 650°C, SEM

The microstructure observed after annealing at 600°C for 100,000 h reveals a partial decay of the lath structure of tempered martensite areas and advanced precipitation process at the former austenite grain boundaries and martensite laths, which manifests itself in the increase (Fig. 7a) and coagulation of precipitates that form chains at the former austenite grain boundaries. The highest degradation level due to long-term exposure at elevated temperature was observed for steel annealed at 650°C – Fig. 7b. This microstructure is characterised by precipitates with the highest diameter and highest decay of the lath structure of martensite.

Table 2.
Classification of changes in the structure of P92 steel after long-term annealing [30]

Material state	Classification of structural changes in accordance with Fig. 12
Initial state	Martensite plates: class 0; precipitates: class o; destruction processes: class 0 material state: CLASS 0; exhaustion degree: 0;
Annealing 1000h/600°C Annealing 1000h/650°C	Martensite plates: class 0/I; precipitates: class o/a; destruction processes: class 0 material state: CLASS 1; exhaustion degree: approx. 0.2
Annealing 10,000h/600°C	Martensite plates: class 0/I; precipitates: class o/a; destruction processes: class 0 material state: CLASS 1; exhaustion degree: approx. 0.2
Annealing 10,000h/650°C	Martensite plates: class 0/I; precipitates: class a; destruction processes: class 0 material state: CLASS 1/2; exhaustion degree: approx. 0.2-0.3
Annealing 30,000h/600°C	Martensite plates: class 0/I; precipitates: class o/a; destruction processes: class 0 material state: CLASS 1; exhaustion degree: approx. 0.2
Annealing 30,000h/650°C Annealing 70,000h/600°C	Martensite plates: class 0/I; precipitates: class a; destruction processes: class 0 material state: CLASS 1/2; exhaustion degree: approx. 0.2-0.3
Annealing 70,000h/650°C	Martensite plates: class I; precipitates: class a; destruction processes: class 0 material state: CLASS 2; exhaustion degree: approx. 0.3
Annealing 100,000h/600°C	Martensite plates: class I; precipitates: class a; destruction processes: class 0 material state: CLASS 2; exhaustion degree: approx. 0.3
Annealing 100,000h/650°C	Martensite plates: class I; precipitates: class a/b; destruction processes: class 0 material state: CLASS 2/3; exhaustion degree: approx. 0.3-0.4

For recorded structure images of P92 steel after long-term annealing the exhaustion degree was assigned (Table 2) based on own classification of the Institute for Ferrous Metallurgy [30].

3.2. Analysis of the increase in the size of particles of P92 steel after exposure at elevated temperature

For the recorded model images of the microstructure of P92 steel, both in initial state and after long-term annealing, the distribution of diameters of the occurred precipitates was determined. The results in the form of distributions of equivalent diameters of precipitates occurring in the analysed states of the tested P92 steel are shown as histograms in Figs. 8-16. These histograms take into consideration the empirical distributions of relative and cumulative frequency.

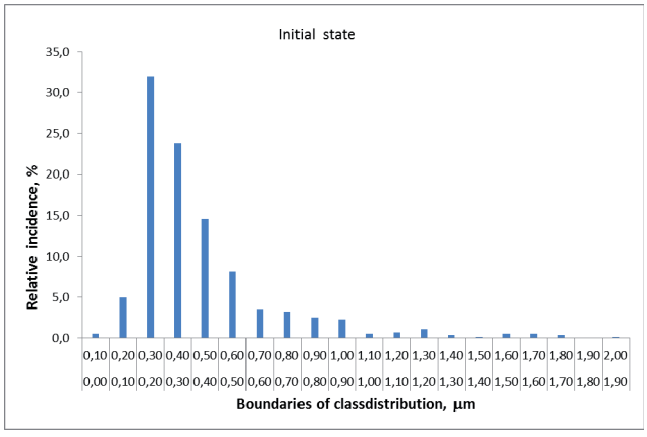

Fig. 8. Chart of empirical distribution of diameters of equivalent particle of the steel in the initial state P92

Changes in the size of particles in P92 steel in initial state and after annealing at 600 and 650°C unanimously indicate that their equivalent diameters increase as the temperature level and time of annealing grow. It was observed that the rate of particle growth at the annealing temperature of 650°C was significantly higher than that at 600°C. It was also observed that at 600°C, which is similar to the expected working temperature, there was a significant increase in mean diameter of precipitates within the time of up to 1,000 h, and the increase was very slow, whereas in case of annealing at 650°C the continuous increase in mean diameter of precipitates was observed depending on the time of annealing (Fig. 16).

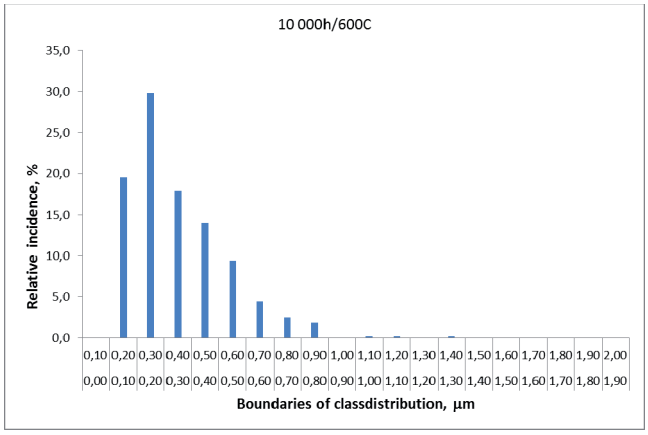

Fig. 9. Chart of empirical distribution of diameters of equivalent particle of P92 steel after annealing 10,000 h/600°C

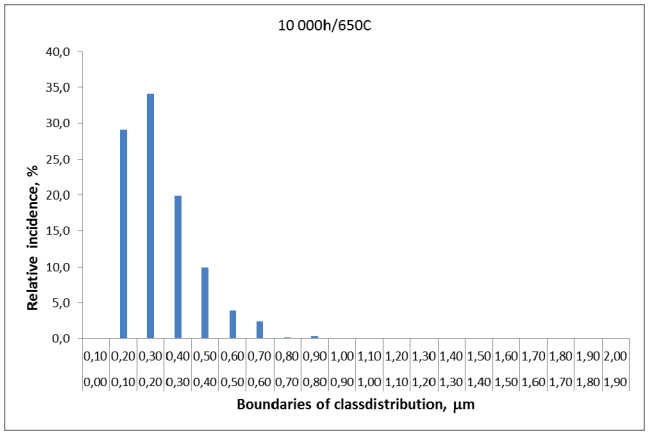

Fig. 10. Chart of empirical distribution of diameters of equivalent particle of P92 steel after annealing 10,000 h/650°C

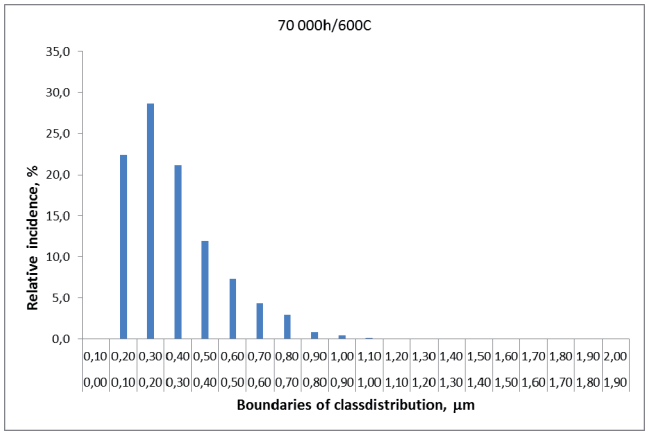

Fig. 11. Chart of empirical distribution of diameters of equivalent particle of P92 steel after annealing 70,000 h/600°C

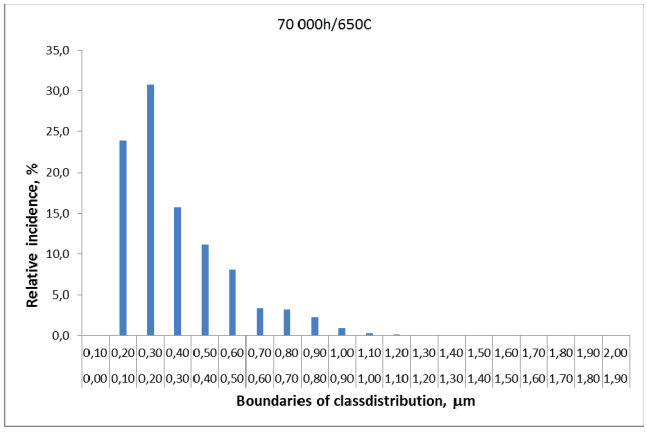

Fig. 12. Chart of empirical distribution of diameters of equivalent particle of P92 steel after annealing 70,000 h/650°C

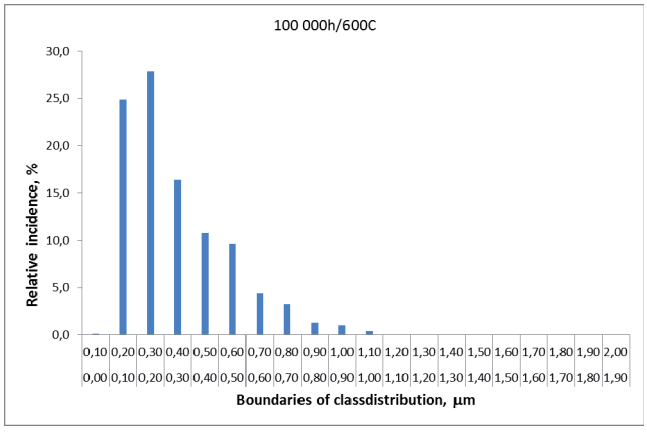

Fig. 13. Chart of empirical distribution of diameters of equivalent particle of P92 steel after annealing 100,000 h/600°C

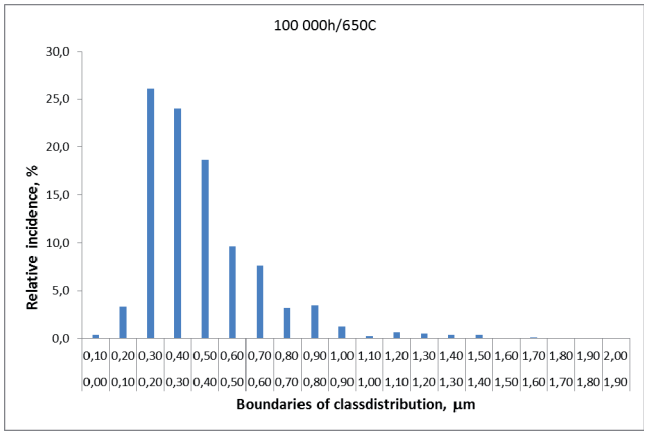

Fig. 14. Chart of empirical distribution of diameters of equivalent particle of P92 steel after annealing 100,000 h/650°C

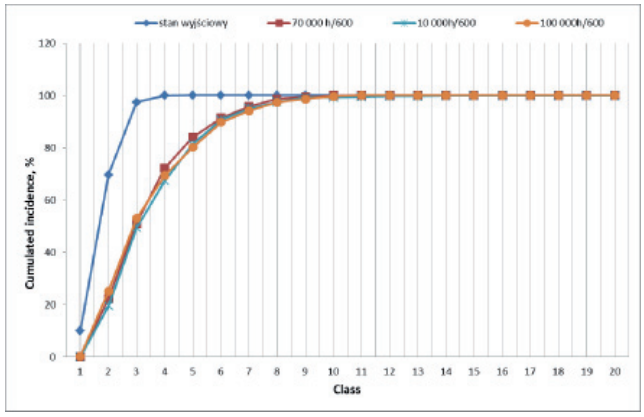

Fig. 15. Specification of cumulative frequency distributions for the precipitates in the steel P92 after long-term annealing at 600°C

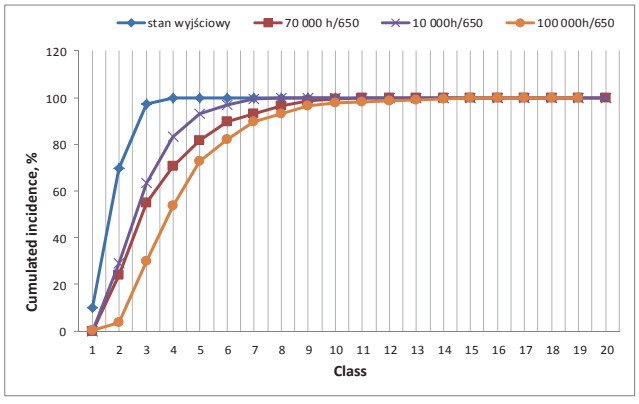

Fig. 16. Specification of cumulative frequency distributions for the precipitates in the steel P92 after long-term annealing at 650°C

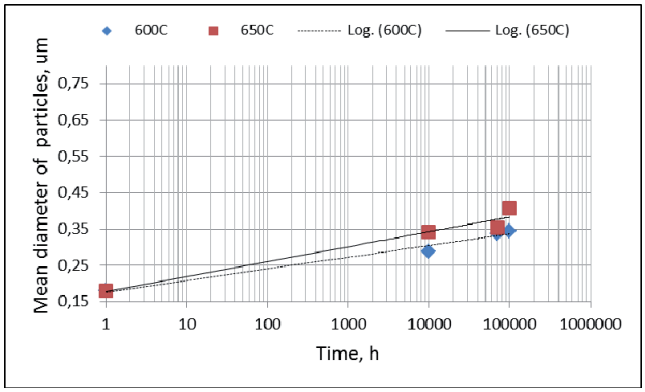

Fig. 17. Diagram of influence of annealing temperature and time on the mean particle diameter of P92 steel

By comparing the obtained test results and the analysis of increase in mean diameter of precipitates, it can be noticed that changes in the size of precipitates after 10,000 h/650°C annealing are similar to the results obtained after 100,000 h annealing at 600°C (Fig. 17).

Table 3 summarises the results of measurements of mean precipitate diameter with reference to time and temperature of annealing. The obtained results were referred to the exhaustion extent of P92 steel in accordance with own classification of the Institute for Ferrous Metallurgy. Thus, the computer-assisted analysis of the image of changes in the size of precipitates is one of the components used in the evaluation of residual life of the tested steel.

The comprehensive evaluation of the exhaustion extent of P92 steel after exposure at elevated temperature should also include the disintegration of martensite structure.

Table 3.
Classification of changes in the structure of P92 steel after long-term annealing with reference to mean diameter of the occurring precipitates

Material state	Mean diameter, μm	Standard deviation	Min. diameter, μm	Max. diameter, μm	Precipitates *	Martensite plates *	Exhaust degree*
Initial state	0.178	0.061	0.063	0.388	o	0	0
10,000 h/600°C	0.289	0.124	0.119	0.878	o/a	0/I	up to 0.2
10,000 h/650°C	0.342	0.180	0.110	1.382	a	0/I	approx. 0.2-0.3
70,000 h/600°C	0.337	0.165	0.110	1.020	a	0/I	approx. 0.2-0.3
70,000 h/650°C	0.354	0.189	0.110	1.133	a	I	approx. 0.3
100,000 h/600°C	0.345	0.186	0.045	1.089	a	0/I	approx. 0.2-0.3
100,000 h/650°C	0.407	0.218	0.090	1.658	a/b	I	approx. 0.3-0.4

* Classification of the Institute for Ferrous Metallurgy [30]

4. Conclusions

The analysis of the image of structure of P92 steel after annealing at 600 and 650°C for up to 1000 hours revealed no essential changes in the microstructure. Further extensions of the time of exposure at elevated temperature results in noticeable changes in the microstructure. The microstructure of P92 steel observed after 100,000 h reveals a partial decay of the lath structure of tempered martensite areas and advanced precipitation processes, especially at the former austenite grain boundaries, resulting in formation of the so-called continuous network of precipitates. The increase in the size of precipitates was revealed, which unambiguously indicated the occurring precipitation coagulation process, with higher dynamics of changes at 650°C.

The confirmation of changes in the structure is the quantitative analysis of the increase in occurring precipitates, which revealed high stability of changes in the structure image at 600°C. It is particularly noticeable in Fig. 15, which presents the specifications of frequency distributions of cumulated precipitates.

The dynamics of changes in the structure due to the increase in temperature is presented in Fig. 17, where sizes of precipitates after 10,000 h/650°C annealing are similar to the results obtained after 100,000 h annealing at 600°C.

The quantitative and qualitative analysis of temperature impact on degradation of mechanical properties and structure of P92 steel is used in the evaluation of changes in functional properties of the material of components working under creep conditions.

References

[1] A. Hernas, Materials and technologies for construction of supercritical boilers and waste incinerators, Joint publication edited by A. Hernas, Katowice 2009, 9.

[2] J. Dobrzański, A. Zieliński, A. Hernas, Structure and properties of new ferritic-based creep-resisting steels, Materials and technologies for construction of supercritical boilers and waste incinerators, Joint publication edited by A. Hernas, Katowice 2009, 48-49.
[3] A. Czyrska-Filemonowicz, A. Zielińska-Lipiec, P.J. Ennis, Modified 9% Cr steels for advanced power generation: microstructure and properties, Journal of Achievements in Materials and Manufacturing Engineering 19/2 (2006) 43-48.
[4] C.G. Panait, A. Zielińska-Lipiec, T. Koziel, A. Czyrska-Filemonowicz, A.F. Gourgues-Lorenzon, W. Bendick, Evolution of dislocation density, size of subgrains and MX-type precipitates in a P91 steel during creep and during thermal ageing at 600°C for more than 100,000 h, Materials Science and Engineering A 527/16 (2010) 4062-4069.
[5] A. Zielińska-Lipiec, The Analysis of Microstructural Stability of Modified Martensitic Deformation, AGH Publishing, Cracow, 2005.
[6] G. Golański, Evolution of Secondary Phases in GX12CrMoVNbN9-1 Cast Steel after Heat Treatment, Archives of Materials Science and Engineering 48/1 (2011) 12-18.
[7] S. Mandziej, A. Vyrostkova, C. Chovet, Microstructure and Creep Rupture of P92-grade weld metal, Welding in the World 55/5-6 (2011) 37-51.
[8] S. Jin, L. Guo, T. Li, J. Chen, Z. Yang, F. Luo, R. Tang, Y. Qiao, F. Liu, Microstructural evolution of P92 ferritic/martensitic steel under Ar^{+} ion irradiation at elevated temperature, Materials Characterization 68 (2012) 63-70.
[9] J. Dobrzański, A. Zieliński, M. Sroka, The influence of simultaneous impact of temperature and time on the properties and structure of X10CrWMoVNb9-2 steel, Journal of Materials Processing Technology 34/1 (2009) 7-14.
[10] M. Sroka, A. Zieliński, Matrix replica method and artificial neural networks as a component of condition assessment of materials for the power industry, Archives of Materials Science and Engineering 58/2 (2012) 130-136.
[11] A. Zieliński, J. Dobrzański, M. Sroka, Changes in the structure of VM12 steel after being exposed to creep conditions, Archives of Materials Science and Engineering 49/2 (2011) 103-111.
[12] G. Golański, Mechanical properties of GX12CrMoVNbN91 (GP91) cast steel after different heat treatments, Materials Science 48/3 (2012) 384-391.
[13] L.A. Dobrzański, M. Sroka, J. Dobrzański, Application of neural networks to classification of internal damages in steels working in creep service, Journal of Achievements in Materials and Manufacturing Engineering 20/1-2 (2007) 303-306.
[14] A. Hernas, J. Dobrzański, Durability and destruction of boiler and steam turbine elements, Publishing House of the Silesian University of Technology, Gliwice, 2003.
[15] J. Dobrzański, Internal damage processes in low alloy chromium–molybdenum steels during high-temperature creep service, Journal of Materials Processing Technology 157 (2004) 297-303.
[16] J. Dobrzański, Diagnostics of damages to pressure components of power devices in assessment of reasons for failures based on materials testing, Transactions of the IMŻ 61/2 (2009) 36-45.
[17] A. Zieliński, G. Golański, A. Zielińska-Lipiec, J. Jasak, C. Kolan, Influence of ageing process on microstructure and mechanical properties of 9%Cr cast steel, Proceedings of the 10th International Conference "Materials for Advanced Power Engineering", Liege, 2014 (in print).
[18] G. Golański, J. Kępa, Role of complex nitride Cr(V, Nb)N – Z phases in high-chromium martensitic steels, Materials Science 32/6 (2011) 917-922.
[19] A. Zieliński, J. Dobrzański, Material properties and structure of thick-walled elements made of steel 7CrMoVTiB10-10 after long-term annealing, Archives of Materials Science and Engineering 58/1 (2012) 5-12.
[20] Data Package for NF616 Ferritic steel (Cr-0,5Mo-1,8W-Nb-V), Nippon Steel Corporation, January 1993.
[21] F. Abe, M.T. Horiuchi, M. Taneike, K. Sawada, Stabilization of martensitic microstructure in advanced 9Cr steel during creep at high temperature, Materials Science and Engineering A 378 (2004) 299-303.
[22] H. Semba, F. Abe, Alloy design and creep strength of advanced 9%Cr USC boiler steels containing high boron, Proceedings of the 8th International Conference "Materials for Advanced Power Engineering", Liege, 2006, 1041-1052.
[23] V. Sklenicka, K. Kucharova, M. Svoboda, L. Kloc, J. Kudrman, Effect of nonsteady loading on creep behaviour of advanced 9-12% fossil power plant steel, Proceedings of the 8th International Conference "Materials for Advanced Power Engineering", Liege, 2006, 1127-1136.
[24] J. Dobrzański, M. Sroka, A. Zieliński, Methodology of classification of internal damage the steels during

creep service, Journal of Achievements in Materials and Manufacturing Engineering 18/1-2 (2006) 263-266.
[25] G. Golański, K. Prusik, P. Wieczorek, Analysis of changes in T91 steel microstructure after long-lasting exploitation, Energetics XVIII (2008)55-56 (in Polish).
[26] B.J. Kim, B.S. Lim, Relationship Between Creep Rupture Life and Microstructure of Aged P92 Steel, Experimental Analysis of Nano and Engineering Materials and Structures, Proceedings of the 13th International Conference "Experimental Mechanics", Alexandroupolis, 2007, 269-270.
[27] A. Zieliński, J. Dobrzański, H. Krztoń, Structural changes in low alloy cast steel Cr-Mo-V after long time creep service, Journal of Achievements in Materials and Manufacturing Engineering 25/1 (2007) 33-36.
[28] C. Chovet, E. Galand, G. Ehrhart, E. Baune, B. Leduey, Welding consumables for grade P92 steel for power generation applications, Safety and reliability of welded components in energy and processing industry, Proceedings of the IIW International Conference, Graz, 2008, 443-448.
[29] PN-EN 10216-2, January 2009, Seamless steel tubes for pressure purposes. Technical delivery conditions. Part 2: Non-alloy and alloy steel tubes with specified elevated temperature properties.
[30] A. Zieliński, J. Dobrzański, H. Paszowska, Changes in the structure and mechanical properties as a result of simultaneous impact of temperature, stress and time of 9-12% Cr steel on critical components of boilers with supercritical parameters working under creep conditions, Transactions of the IMŻ 62 (2011) 60-62.
[31] J. Dobrzański, M. Sroka, Computer aided classification of internal damages the chromium-molybdenum steels after creep service, Journal of Achievements in Materials and Manufacturing Engineering 24/2 (2007) 143-146.
[32] J. Dobrzański, A. Zieliński, M. Sroka, Structure, properties and method of the state evaluation of low-alloyed steel T23 (HCM2S) worked in creep conditions, Proceedings of the 11th International Scientific Conference "Contemporary Achievements in Mechanics, Manufacturing and Materials Science" CAM3S'2005, Gliwice-Zakopane, 2005, 4-7.